JOURNAL OF CHEMICAL & ENGINEERING DATA

ARTICLE

pubs.acs.org/jced

Density and Viscosity of Aqueous (Piperazine + Carbon Dioxide) Solutions

Stephanie A. Freeman and Gary T. Rochelle*

Department of Chemical Engineering, The University of Texas at Austin, 1 University Station C0400, Austin Texas 78712, United States

ABSTRACT: The density (ρ) and viscosity (μ) of aqueous (piperazine (PZ) + carbon dioxide (CO_2)) solutions were measured over a temperature range of (293.15 to 333.15) K and concentration ranges of (1.5 to 7.0) $mol \cdot kg^{-1}$ PZ ((2 to 20) molal (m) PZ) and (0 to 4.0) $mol \cdot kg^{-1}$ CO_2. Data for density and viscosity are presented in tabular form and include units useful for CO_2 capture applications (CO_2 loading and PZ concentration in m). Density data are analyzed as the ratio of ρ to the density of water to eliminate the effect of temperature. On this basis, ρ for (5 to 12) m PZ ((3.2 to 5.0) $mol \cdot kg^{-1}$ PZ) was correlated with a linear regression as a function of CO_2 and PZ concentrations to within 0.78 % for all data. A prediction of ρ up to 20 m PZ induces an error of only 1.5 %. Viscosity data are analyzed in a similar way, and a regression for 8 m PZ (4.1 $mol \cdot kg^{-1}$ PZ) viscosity fit all experimental data within 6.0 %. The applicability of these regressions to online monitoring of a PZ based CO_2 capture application is discussed.

INTRODUCTION

Amine-based absorption-stripping for CO_2 capture from coal-fired power plant flue gas will be an important technology to address global climate change. Concentrated aqueous piperazine (PZ) has been identified as an attractive solvent for this process.[1,2] The physical properties of any solvent used in a amine-based absorption-stripping system are critical to understanding the thermodynamics, hydrodynamics, and optimum operating conditions. The density and viscosity of PZ solutions are needed for design calculations of fluid flow and heat transfer. Because high viscosity interferes with mass transfer and increases the size of heat exchangers, the maximum concentration of PZ in the solvent may be determined by its viscosity.

Online viscosity and density monitors can be employed in a pilot plant, demonstration plant, or full scale CO_2 capture application as an inexpensive, easy, and effective way to continually monitor the condition of an amine solvent. Chen[3] and Dugas[4] demonstrated that online density measurements were useful in inferring CO_2 loading of potassium carbonate promoted by PZ and monoethanolamine (MEA) solutions during pilot plant operations. Both PZ concentration and CO_2 loading have traditionally been offline analyses that take on the order of minutes or hours to complete. Online monitoring allows for instant feedback and constant monitoring of the solvent conditions where maintaining the solution within physical solubility windows is a crucial operational concern.

PZ has been investigated as a CO_2 rate promoter in solvents primarily consisting of aqueous methyldiethanolamine (MDEA),[5−12] 2-amino-2-methyl-1-propanol (AMP),[6,13−15] or potassium carbonate.[16−20] Concentrated PZ (40 wt %) has also been explored as a standalone solvent for CO_2 capture.[1,2,21] PZ has a low solubility in water which can prove detrimental in a large scale system and discouraged research into the solvent. The solubility of the PZ + H_2O system has been investigated previously,[8,22,23] but the effect of adding CO_2 to the system has only been researched recently.[2,23] Large-scale CO_2 capture systems will contain a wide range of CO_2 concentrations throughout the absorber, stripper, and other unit operations; therefore, a full understanding of the effect of CO_2 concentration on the physical properties of a solvent is crucial. Previous literature on the density and viscosity of PZ solutions only included data at low PZ concentrations to avoid solutions that were slurries or contained solids.[24−27] The concentrations of PZ studied, always less than 14 wt % at 20 °C, are not useful for CO_2 capture applications since they cannot compete with the CO_2 capture capacity of a baseline MEA solvent.

Recently, the addition of CO_2 to an aqueous solution of PZ was found to reduce solubility concerns as PZ carbamate ($PZCOO^-$) is more soluble than anhydrous PZ itself.[2,23] Concentrated solutions can be made without insolubility and have been shown to have very advantageous properties for CO_2 capture such as a fast rate of CO_2 absorption, high capacity, and resistance to thermal and oxidative degradation.[1,2] Physical property studies that include PZ in the presence of CO_2 report on a blended solution with another amine, such as MDEA or AMP, where PZ is added as a kinetic promoter.[12] In the few studies where the PZ + H_2O + CO_2 system is investigated alone, the only properties measured and reported are CO_2 solubility, N_2O solubility, Henry's constants, and diffusivities.[23,28] Literature data for the density and viscosity of PZ solutions in the presence of CO_2 are not available outside of the author's previous work.[2]

This study provides density and viscosity data over ranges of PZ and CO_2 concentrations applicable to CO_2 capture applications. To match with previous CO_2 capture solvent literature, solutions are analyzed at (2 to 20) molal (m) PZ and a CO_2 loading of 0 to 0.47 $(mol\ CO_2) \cdot (mol\ alkalinity)^{-1}$. The data are reported in SI concentration units ($mol \cdot kg^{-1}$), but other common units are also provided (i.e., m and CO_2 loading) for clarity to the readers in this field. The data are not all-inclusive

Received: November 15, 2010
Accepted: January 20, 2011
Published: February 14, 2011

Table 1. Density (ρ) of Aqueous ($PZ + CO_2$) Solutions at T/K = 293.15, 313.15, and 333.15

C_{PZ}	C_{PZ}	C_{CO_2}	C_{CO_2}	ρ/kg·m^{-3}		
m	mol·kg^{-1}	mol·(mol alk)$^{-1}$	mol·kg^{-1}	T/K = 293.15	T/K = 313.15	T/K = 333.15
2	1.67	0.00	0.000	1006.7	999.4	989.1
	1.64	0.05	0.186	1014.6	1007.2	997.4
	1.64	0.11	0.366	1022.2	1014.8	1004.9
	1.63	0.16	0.545	1029.9	1022.4	1012.9
	1.61	0.22	0.728	1037.3	1029.9	1020.2
	1.61	0.25	0.894	1044.1	1036.5	1027.0
	1.59	0.32	1.080	1051.5	1043.8	1034.4
	1.58	0.38	1.246	1058.1	1050.5	1040.7
	1.57	0.44	1.416	1064.4	1056.7	-
	1.55	0.47	1.516	1068.8	1060.7	-
5	3.36	0.11	0.753	1049.3	-	-
	3.33	0.15	0.991	1062.2	1052.6	-
	3.25	0.22	1.433	1074.9	1065.5	1054.8
	3.21	0.28	1.780	1087.4	1078.2	1067.6
	3.16	0.35	2.216	1099.2	1090.2	1079.9
	3.11	0.40	2.504	1111.1	1102.1	1092.0
	3.06	0.46	2.822	1122.3	1113.3	1103.1
	3.03	0.50	3.023	1127.8	1118.8	1108.1
	3.01	0.53	3.182	1136.9	1127.6	-
7	4.11	0.16	1.281	1076.9	1066.1	-
	4.01	0.21	1.726	1092.3	1082.1	1070.7
	3.93	0.26	2.091	1106.1	1096.1	1085.2
	3.86	0.32	2.495	1120.6	1110.9	1100.4
	3.81	0.37	2.815	1134.1	1124.6	1114.3
	3.72	0.40	3.023	1147.3	1137.9	1127.7
	3.68	0.46	3.397	1159.6	1150.1	-
8	4.28	0.20	1.722	1100.7	1090.0	1078.5
	4.26	0.25	2.150	1116.2	1105.9	1094.9
	4.12	0.31	2.563	1130.8	1121.3	1110.7
	4.11	0.35	2.917	1145.7	1136.0	1125.7
	3.98	0.41	3.297	1160.1	1150.4	1140.2
	3.90	0.45	3.617	1173.4	1163.8	-
9	4.68	0.15	1.453	1090.9	-	-
	4.59	0.20	1.879	1107.0	1096.1	1084.3
	4.52	0.26	2.347	1123.4	1112.8	1101.7
	4.41	0.30	2.714	1137.2	1127.0	1116.3
	4.33	0.36	3.169	1155.2	1145.3	1134.9
	4.24	0.40	3.471	1168.7	1158.9	1148.7
	4.14	0.44	3.695	1181.6	1171.7	-
10	4.80	0.25	2.436	1132.3	1121.2	1110.0
	4.73	0.31	2.875	1149.0	1138.7	1127.8
	4.69	0.36	3.343	1165.0	1154.9	1144.6
	4.41	0.41	3.726	1180.7	1170.8	1160.5
12	5.23	0.20	2.650	1121.9	1110.1	1097.8
	5.07	0.26	2.697	1139.8	1128.3	1116.7
	4.96	0.31	3.169	1156.9	1146.2	1135.3
	4.85	0.36	3.620	1173.6	1163.2	1152.7
	4.73	0.41	3.985	1189.5	1179.3	1169.0
20	6.96	0.10	1.338	1100.6	1084.7	1069.3
	6.70	0.16	2.123	1125.6	1110.8	1096.2
	6.53	0.20	2.577	1145.3	1131.3	1118.8
	6.47	0.25	3.137	1166.4	1153.7	1141.0

Table 2. Viscosity (μ) of Aqueous (PZ + CO_2) Solutions at T/K = 298.15, 313.15, and 333.15

C_{PZ}	C_{PZ}	C_{CO_2}	C_{CO_2}	μ/mPa·s								
m	mol·kg^{-1}	mol·(mol alk)$^{-1}$	mol·kg^{-1}	T/K = 298.15			T/K = 313.15			T/K = 333.15		
2	1.67	0.00	0.000	1.877	±	0.011	1.307	±	0.016	0.895	±	0.016
	1.64	0.05	0.186	1.896	±	0.007	1.334	±	0.014	0.906	±	0.020
	1.64	0.11	0.366	1.910	±	0.008	1.348	±	0.018	0.933	±	0.020
	1.63	0.16	0.545	1.917	±	0.008	1.371	±	0.015	0.942	±	0.018
	1.61	0.22	0.728	1.930	±	0.009	1.386	±	0.013	0.984	±	0.017
	1.61	0.25	0.894	1.952	±	0.006	1.414	±	0.018	0.984	±	0.018
	1.59	0.32	1.080	1.961	±	0.007	1.423	±	0.016	1.015	±	0.017
	1.58	0.38	1.246	1.971	±	0.010	1.439	±	0.011	1.021	±	0.017
	1.57	0.44	1.416	1.977	±	0.009	1.455	±	0.014	1.043	±	0.029
	1.55	0.47	1.516	1.968	±	0.013	1.468	±	0.041	-	-	-
5	3.25	0.22	1.433	-	-	-	3.231	±	0.012	1.946	±	0.018
	3.21	0.28	1.780	5.336	±	0.039	3.346	±	0.015	2.028	±	0.019
	3.16	0.35	2.216	5.457	±	0.022	3.464	±	0.007	2.144	±	0.021
	3.11	0.40	2.504	5.872	±	0.018	3.612	±	0.011	2.230	±	0.023
	3.06	0.46	2.822	5.927	±	0.015	3.689	±	0.014	2.309	±	0.019
	3.03	0.50	3.023	5.941	±	0.014	3.752	±	0.014	2.366	±	0.033
	3.01	0.53	3.182	6.010	±	0.018	3.751	±	0.010	2.502	±	0.022
7	4.01	0.21	1.726	10.85	±	0.053	6.347	±	0.039	3.543	±	0.050
	3.93	0.26	2.091	11.34	±	0.052	6.484	±	0.053	3.720	±	0.058
	3.86	0.32	2.495	11.60	±	0.000	6.929	±	0.070	4.218	±	0.057
	3.81	0.37	2.815	12.34	±	0.052	7.222	±	0.076	4.810	±	0.216
	3.72	0.40	3.023	12.60	±	0.047	7.617	±	0.082	4.849	±	0.104
	3.68	0.46	3.397	12.82	±	0.063	7.854	±	0.094	5.270	±	0.243
9	4.59	0.20	1.879	20.82	±	0.042	11.09	±	0.088	5.659	±	0.036
	4.52	0.26	2.347	22.03	±	0.048	12.09	±	0.120	6.318	±	0.060
	4.41	0.30	2.714	23.10	±	0.047	12.60	±	0.105	7.562	±	0.143
	4.33	0.36	3.169	23.99	±	0.032	13.90	±	0.115	8.442	±	0.186
	4.24	0.40	3.471	25.34	±	0.052	14.62	±	0.132	9.162	±	0.214
	4.14	0.44	3.695	26.72	±	0.079	15.21	±	0.110	10.24	±	0.466
10	4.80	0.25	2.436	31.37	±	0.189	16.92	±	0.253	9.084	±	0.069
	4.73	0.31	2.875	33.42	±	0.220	18.08	±	0.210	9.781	±	0.342
	4.69	0.36	3.343	35.45	±	0.227	19.89	±	0.407	11.06	±	0.237
	4.41	0.41	3.726	37.48	±	0.352	21.18	±	0.239	11.88	±	0.352
12	5.23	0.20	2.650	49.35	±	0.127	23.62	±	0.286	10.22	±	0.162
	5.07	0.26	2.697	52.68	±	0.181	26.01	±	0.213	11.78	±	0.294
	4.96	0.31	3.169	57.22	±	0.297	27.18	±	0.215	13.34	±	0.255
	4.85	0.36	3.620	60.17	±	0.236	31.42	±	0.413	15.11	±	0.213
	4.73	0.41	3.985	63.22	±	0.361	33.43	±	0.316	18.32	±	0.290
20	6.70	0.16	2.123	304.1	±	0.994	95.61	±	0.357	30.00	±	0.176
	6.53	0.20	2.577	373.1	±	0.994	120.3	±	0.483	40.88	±	0.286
	6.47	0.25	3.137	534.3	±	2.058	138.9	±	0.994	57.14	±	0.420

across a range of CO_2 concentrations for a given PZ concentration and are absent where PZ precipitation or CO_2 evolution occurred.

EXPERIMENTAL SECTION

Solution Preparation. Aqueous solutions were prepared as described previously by heating anhydrous PZ (IUPAC: 1,4-diazacyclohexane, CAS 110-85-0, purity 99 %, Acros Organics N. V., Geel, Belgium) in distilled, deionized water.[1,2,23] Once the solid PZ flakes were dissolved, the PZ solution was transferred to a gas washing bottle where CO_2 (CAS 124-38-9, purity 99.5 %, Matheson Tri Gas, Basking Ridge, NJ) was gravimetrically sparged to achieve the desired CO_2 concentration. The PZ concentration was determined by acid titration,[23] and the CO_2 concentration was determined by total inorganic carbon (TIC) analysis.[23]

PZ Concentration through Acid Titration. An automatic Titrando series titrator with equivalence point detection and controlled dosing (Metrohm USA, Riverview, FL, USA) was used as described previously to measure total amine concentration for each solution at room temperature (T = 293.15 K).[23]

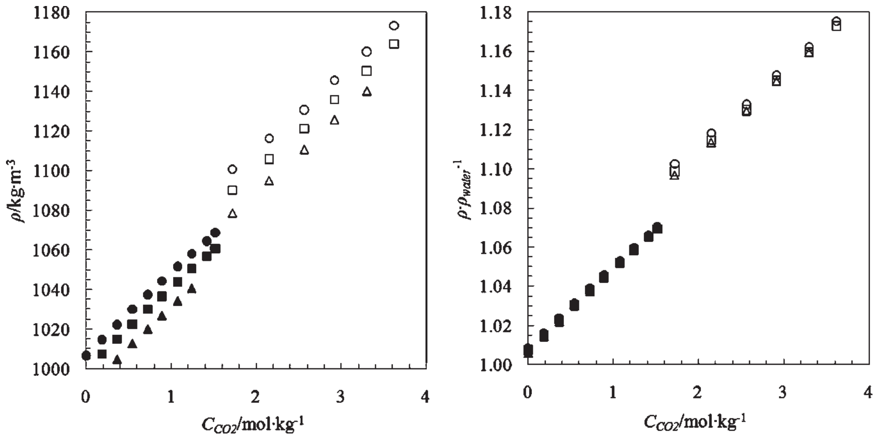

Figure 1. Density (ρ) (left panel) and $\rho \cdot \rho_{\text{water}}$ (right panel) as a function of CO_2 concentration for aqueous PZ solutions. For 2 *m* PZ: ●, $T = 293.15$ K; ■, $T = 313.15$ K; ▲, $T = 333.15$ K. For 8 *m* PZ: ○, $T = 293.15$ K; □, $T = 313.15$ K; △, $T = 333.15$ K.

Samples were diluted 300× in analytical grade water and titrated with 0.2 $\text{mol} \cdot \text{dm}^{-1}$ H_2SO_4 to a final pH of 2.4, past the final equivalence point. Two equivalence points were automatically detected for PZ that correspond to the protonation of each amino function. The second equivalence point, representing the equilibrium between mono- and diprotonated PZ (H^+PZ/H^+PZH^+), generally occurred at a pH 3.9 and was used for the amine concentration calculations. The amine concentration by titration was consistently about 2.0 % less than that from the gravimetric preparation.

CO_2 Concentration through Total Inorganic Carbon (TIC). The CO_2 concentration was measured using TIC analysis as described previously.[1,2,23] Samples were diluted 100× in analytical grade water before injection into the TIC. Samples were acidified in 2.6 M H_3PO_4 in the injection cell of the TIC to shift the equilibrium of all CO_2 containing species to gaseous CO_2. A stream of nitrogen carried the released CO_2 through two drying tubes to an infrared CO_2 analyzer (Horiba Instruments Inc., Irving, CA). Injections produced peaks that were integrated and compared to peaks produced from a carbon standard (1000 ppm carbon, Ricca Chemical, Pequannock, NJ) over the range of interest. Every sample was analyzed in triplicate, and an average concentration was calculated.

The loading analysis is the most imprecise part of this study. The loading of amine solutions can be change greatly due to handling, opening of bottles, or age of samples. All samples were handled carefully and analyzed immediately, but the loading of solutions inherently changed during the course of density and viscosity measurements. The error of the density and viscosity measurements is very low compared with the error in the measurement of CO_2 concentration. The estimated error in the TIC measurement is 4.0 %. Instrument errors are reported for the density meter and viscometer, but the error in CO_2 concentration overshadows them and has the most impact on the data regressions.

Density. Density was measured in a Mettler-Toledo DE40 density meter (Mettler-Toledo Inc., Columbus, OH, USA). The DE40 achieves precise temperature control using a Peltier thermostat for temperature control within ± 0.01 °C. Calibration is performed at each temperature with dry air and degassed water. Each measurement equilibrates at the desired temperature within 0.01 °C before finalizing a measurement. The repeatability and resolution of the DE40 are 0.1 $\text{kg} \cdot \text{m}^{-3}$. Data are missing at low CO_2 concentrations where solutions could not be analyzed due to PZ precipitation. Data are missing at high CO_2 concentrations where CO_2 evolved from the sample. The higher temperatures of these measurements caused an increased CO_2 partial pressure leading to CO_2 evolution and instability in the measurement. This was evidenced by the production of bubbles visible in the u-tube of the DE40.

Viscosity. Viscosity was measured in a Physica MCR 300 cone-and-plate rheometer with a CP-50 cone (Anton-Paar US, Ashland, VA, USA). The MCR 300 has precise temperature control of the plate using circulating fluid that maintains the plate within 0.01 °C. Samples are measured with a gap of 0.05 mm, and the gap height was verified at each temperature through a zero gap procedure. The angular speed of the cone was varied over from (100 to 1000) s^{-1}. The estimated uncertainty in the measurement of viscosity is 1.0 %.

A total of 10 measurements were taken every 10 s for each sample. Values reported are an average and standard deviation of these 10 instances (Table 2). The percent error represented by the calculated standard deviations ranged from 0.13 % to 4.6 %. Errors were higher at higher temperatures where the value of viscosity was smaller, amplifying the standard deviation value when calculated as a percent.

As with the density measurement, data are not reported at the lower temperature and low CO_2 concentration where precipitation occurred or at the higher temperature and high CO_2 concentration where CO_2 evolved during the measurement. When precipitation occurred, the shear stress during the 10 measurements was nonlinear, producing scatter in the calculated viscosity. The shear stress was very high as the samples were essentially a slurry. At the higher temperatures, the evolution of CO_2 was evidenced by the presence of bubbles before or after the sample was analyzed.

■ RESULTS AND DISCUSSION

Density. The experimental values for the density (ρ) of aqueous ($PZ + CO_2$) solutions as a function of PZ concentration (C_{PZ}), CO_2 concentration (C_{CO_2}), and temperature (T) are listed in Table 1. C_{PZ} is provided in units of *m* and $\text{mol} \cdot \text{kg}^{-1}$. C_{CO_2} is listed in units of $(\text{mol } CO_2) \cdot (\text{mol alk})^{-1}$ and $\text{mol} \cdot \text{kg}^{-1}$. Raw ρ data are provided with the units of $\text{kg} \cdot \text{m}^{-3}$, but the ratio of ρ to the density of water (ρ_{water}) is used throughout the

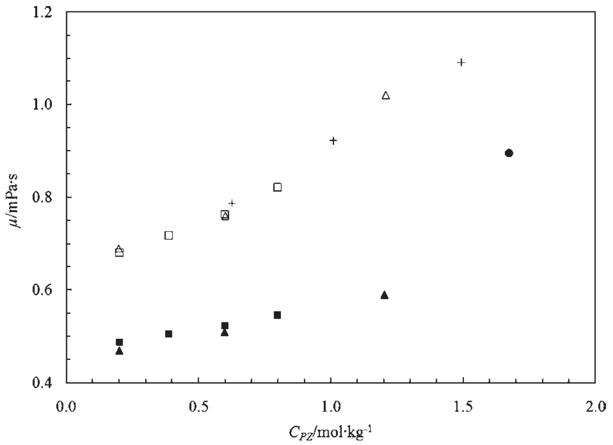

Figure 2. Density (ρ) of PZ without CO_2. At T = 313.15 K: ○, this study; □, ref 27; △, ref 26; +, ref 25; At T = 333.15 K: ●, this study; ■, ref 27; ▲, ref 26.

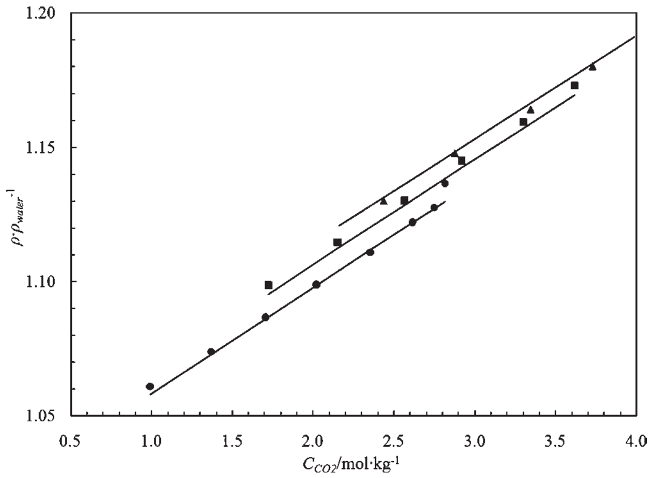

Figure 3. Comparison of $\rho \cdot \rho_{\text{water}}^{-1}$ to the correlation of eq 1 at T = 313.15 K. Data: ●, 5 m PZ; ■, 8 m PZ; ▲, 12 m PZ. Lines: eq 1 for (5, 8, and 12) m PZ.

proceeding discussion, which is unitless. Values for ρ_{water} over the range of T = (293.15 to 333.15) K were taken from the DIPPR Database.[29]

The ratio $\rho \cdot \rho_{\text{water}}^{-1}$ is used to eliminate the temperature dependence of the data. At a given temperature, this ratio does not affect the trends observed. However, over a range of temperature the data collapse and amplify the effect of C_{CO_2} in relation to the effect of T/K on ρ. To demonstrate this effect, the temperature dependence of ρ and $\rho \cdot \rho_{\text{water}}^{-1}$ are shown in Figure 1 for (2 and 8) m PZ ((1.6 and 4.1) mol·kg^{-1} PZ). The advantage of reporting $\rho \cdot \rho_{\text{water}}^{-1}$ rather than ρ is that the effect of temperature can be minimized to focus on the effect of CO_2 concentration. This is a critical observation because the intent is to use online density meters in a CO_2 capture process to monitor CO_2 concentration. With regressions that eliminate the effect of temperature, the CO_2 concentration can be directly related to the density of the solution, allowing simple and direct online monitoring of CO_2 loading throughout a process.

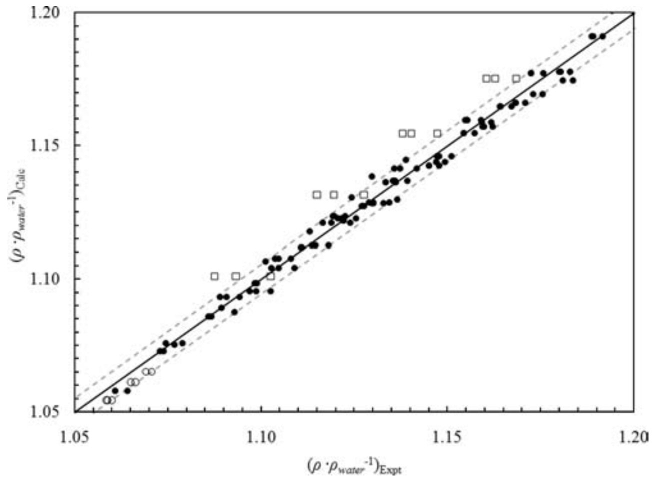

Figure 4. Parity plot demonstrating the accuracy of eq 1 for regressing $\rho \cdot \rho_{\text{water}}^{-1}$ at T = (295.15 to 333.15) K. Data: ●, (5 to 12) m PZ; ○, 2 m PZ; □, 20 m PZ. Lines: solid, $y = x$; dashed, 0.5 % of $y = x$.

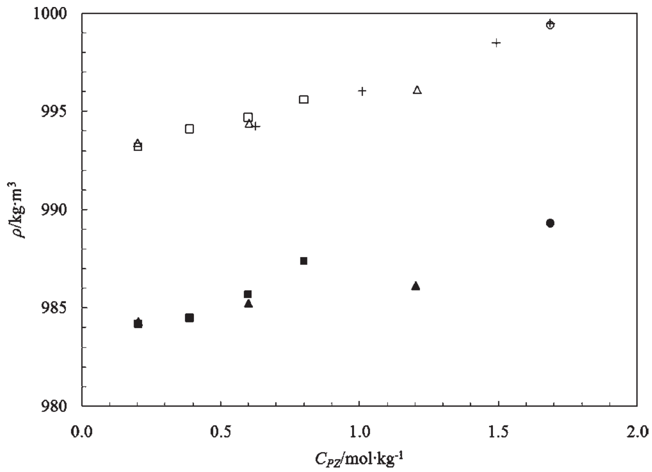

Figure 5. Viscosity (μ) of PZ without CO_2. At T = 313.15 K: ○, this study; □, ref 27; △, ref 26; +, ref 25. At T = 333.15 K: ●, this study; ■, ref 27; ▲, ref 26.

All previous literature data report density in the absence of CO_2, and only the 2 m PZ solution of this study does not precipitate in the absence of CO_2. All other density data reported in this manuscript contain CO_2. The density of 2 m PZ without CO_2 is shown along with previous literature data in Figure 2.[25−27] The data of this study agree with literature values at T = 313.15 K. At T = 333.15 K, the data of Samanta and Bandyopadhyay[27] appear to deviate at their highest PZ concentration, while the data presented in this study agrees with that of Muhammed and colleagues.[26]

The $\rho \cdot \rho_{\text{water}}^{-1}$ of (5, 8, and 12) m PZ at T = 313.15 K are shown as a function of CO_2 concentration in Figure 3. There is not a significant difference in the $\rho \cdot \rho_{\text{water}}^{-1}$ of (5 to 12) m PZ when plotted in these units. The data collapse when observed in terms of $\rho \cdot \rho_{\text{water}}^{-1}$ and C_{CO_2}/mol·kg^{-1}, rather than ρ/kg·m^{-3} and C_{CO_2}/mol·(mol alk)$^{-1}$.

The values for $\rho \cdot \rho_{\text{water}}^{-1}$ for 5 to 12 m PZ were regressed over T = (293.15 to 333.15) K using the least-squares method as a function of C_{CO_2}/mol·kg^{-1} and C_{PZ}/mol·kg^{-1}. The resulting regression is

$$\frac{\rho}{\rho_{\text{water}}} = 0.0407 \cdot C_{CO_2} + 0.008 \cdot C_{PZ} + 0.991 \qquad (1)$$

Table 3. Viscosity of 8 *m* PZ from T/K = 293.15 to 343.15

C_{PZ}	C_{CO_2}	C_{CO_2}	μ/mPa·s						
mol·kg^{-1}	mol·(mol alk)$^{-1}$	mol·kg^{-1}	293.15 K	298.15 K	303.15 K	313.15 K	323.15 K	333.15 K	343.15 K
4.26	0.24	2.150	20.30	16.50	12.93	9.460	6.586	5.351	3.919
4.12	0.29	2.563	20.93	17.14	13.54	9.988	7.072	5.769	4.509
4.11	0.35	2.917	22.21	18.19	14.56	10.79	7.580	6.466	4.683
3.98	0.40	3.297	22.78	18.76	15.24	11.37	8.322	6.905	5.152

Table 4. Value of Parameters in eq 3

parameter	i = 1	i = 2
a	1.723	
b	2.63	−778
c	−1.019	355.16
d	−0.527	169.3

where the standard error in the two coefficients and intercept were 0.00048 kg·(mol CO$_2$)$^{-1}$, 0.00057 kg·(mol PZ)$^{-1}$, and 0.002, respectively. The average error of the total data set was 0.24 %, and the maximum error was 0.78 %. The regression correlates $\rho\cdot\rho_{\text{water}}^{-1}$ with similar accuracy across all three temperatures as the maximum error was 0.78 %, 0.60 %, and 0.49 % for data at T = 293.15 K, 313.15 K, and 333.15 K, respectively. The error in correlating ρ/kg·m^{-3} rather than $\rho\cdot\rho_{\text{water}}^{-1}$ is the same given the nature of the ratio used in the regression. The average absolute deviation (AAD) of a data set is defined as

$$\text{AAD} = \frac{1}{N}\sum_{i=1}^{N}\frac{|y_{\text{calc},i} - y_{\text{expt},i}|}{y_{\text{expt},i}} \tag{2}$$

where $y_{\text{calc},i}$ and $y_{\text{expt},i}$ are the calculated and experiment values, respectively, of the dependent variable of interest, y, and N is the total number of data points. Using eq 2, the AAD of eq 1 with the density data for (5 to 12) *m* PZ at all temperatures was 0.0024, indicating that eq 1 represents the data well.

The experimental $\rho\cdot\rho_{\text{water}}^{-1}$ data at T = 313.15 K are compared with the regression (eq 1) in Figure 3. The correlation of eq 1 is shown for (5, 8, and 12) *m* data to demonstrate the fit to the experimental data without cluttering the figure. The regression (eq 1) did not include data from (2 and 20) *m* PZ because that extremely low or high PZ concentration is not likely to be seen in an industrial system. The concentration of interest is 8 *m* PZ, and the error in the regression was reduced by focusing on PZ concentrations close to 8 *m* PZ. Although the regression does not include (2 and 20) *m* PZ, prediction of these concentrations from eq 1 yields an average error of 0.57 % and a maximum error of 1.48 %. The robustness of eq 1 is demonstrated in the low error obtained when predicting data outside of the concentration ranges of data that were included in the original regression.

Only data at T = 313.15 K are shown in Figure 3 for clarity and because of the importance of this temperature in the absorber side of an absorption-stripping CO$_2$ capture system. To encompass the entire data set, a parity plot comparing the experimental data to the regression of $\rho\cdot\rho_{\text{water}}^{-1}$ from eq 1 for T = (293.15 to 333.15) K and all PZ concentrations is shown in Figure 4. The data for 2 and 20 *m* PZ are highlighted with open points to demonstrate the error in predicting outside of the data used for eq 1.

Viscosity. The measured viscosity (μ) of aqueous (PZ + CO$_2$) as a function of C_{PZ}, C_{CO_2}, and T is given in Table 2. As with density measurements, previous literature has only reported viscosity of aqueous PZ solutions at low concentrations without CO$_2$. Therefore, the only data from this study that are comparable to literature is a 2 *m* PZ solution in the absence of CO$_2$. The viscosity of this solution is compared with previous data in Figure 5 as a function of C_{PZ}/mol·kg^{-1}.[25−27] The viscosity data at T = 313.15 K are in agreement with literature values. At T = 333.15 K, Muhammed and colleagues[26] found lower μ in comparison with the current study at higher C_{PZ}/mol·kg^{-1}. There are no literature data at T = 333.15 K above a C_{PZ}/mol·kg^{-1} of 1.25, so it is not clear if the literature data or the current study predicts the more accurate trend. The density comparison in Figure 2 showed that the current study matched the results of Muhammed and colleagues,[26] while that of Samanta and Bandyopadhyay[27] appeared to deviate with increasing PZ concentration at T = 333.15 K.

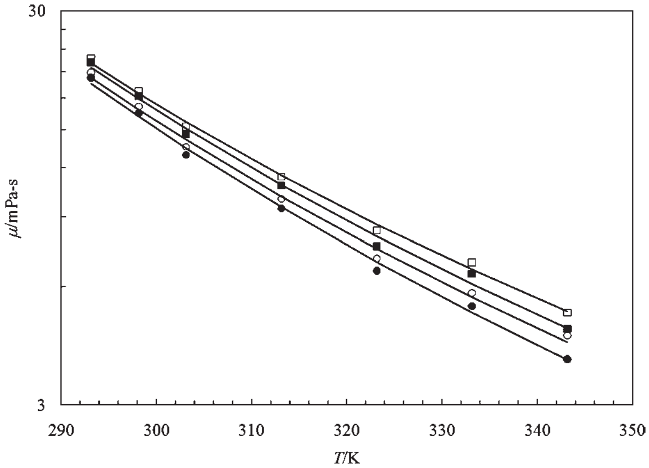

Figure 6. Comparison of the viscosity (μ) of 8 *m* PZ to the correlation of eq 5. Data are varying C_{CO_2}/mol·kg^{-1}: ●, 2.15; ○, 2.56; ■, 2.92; □, 3.30. Lines: eq 3.

An extended set of viscosity data for 8 *m* PZ was obtained over a wider range of temperature than the other PZ concentrations, and the data are shown in Table 3. The importance of 8 *m* PZ in planned and future industrial applications called for a wider range of data and a correlation to predict viscosity for this concentration. A correlation was created from the 8 *m* PZ data to relate the ratio of viscosity to the viscosity of water ($\mu\cdot\mu_{\text{water}}^{-1}$) to T/K, C_{CO_2}/mol·kg^{-1}, and C_{PZ}/mol·kg^{-1}, and has the form of

$$\ln\left(\frac{\mu}{\mu_{\text{water}}}\right) = a_1 + \Phi_1 + \frac{\Phi_2}{T} \tag{3}$$

where

$$\Phi_i = b_i\cdot C_{CO_2} + c_i\cdot C_{PZ} + d_i\cdot C_{CO_2}\cdot C_{PZ} \tag{4}$$

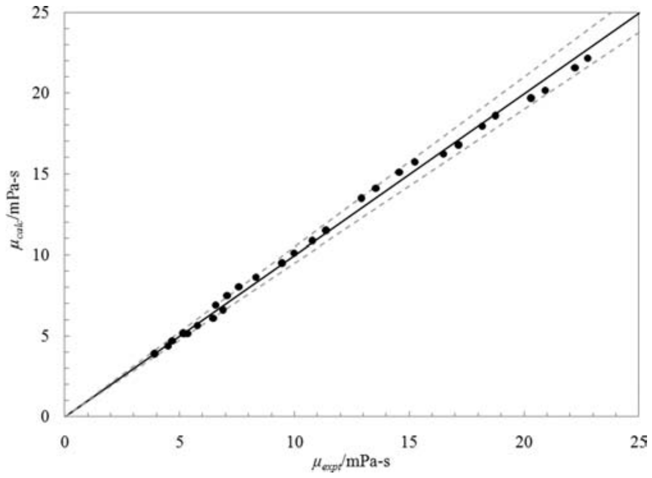

Figure 7. Parity plot demonstrating the accuracy of eq 3 for regressing viscosity (μ) of 8 *m* PZ solutions at T = (293.15 to 343.15) K. Lines: solid, $y = x$; dashed, 5 % of $y = x$.

The values of the regressed parameters can be found in Table 4. Values for μ_{water} over the range of T = (283.15 to 343.15) K were taken from the DIPPR Database.[29] The resulting correlation (eq 3) was able to fit all experimental $\mu \cdot \mu_{\text{water}}^{-1}$ data within 2.4 %. The average absolute deviation (AAD) calculated using eq 2 for the correlation of viscosity data was 0.028 indicating the data set is well-represented by eq 3. Rearranging the above regression (eq 3) for μ as the dependent variable leaves a relationship which correlates the viscosity of 8 *m* PZ with an average deviation of less than 3 % (maximum deviation of 6 %).

The experimental μ/mPa·s data from Table 3 are compared to the correlation of eq 3 in Figure 6. A parity plot comparing the experimental μ/mPa·s data to the values correlated using eq 3 is shown in Figure 7 with 5 % deviation shown with dashed lines.

CONCLUSIONS

Two regressions have been developed for density and viscosity that provide a real solution for online monitoring of PZ systems in industrial use. Equations 2 and 3 are regressions for ρ/kg·m^{-3} and μ/mPa·s as a function of ρ_{water}/kg·m^{-3} or μ_{water}/mPa·s, T, C_{CO_2}/mol·kg^{-1}, and C_{PZ}/mol·kg^{-1}. This presents a system of two equations with two unknowns at any given time, C_{CO_2}/mol·kg^{-1} and C_{PZ}/mol·kg^{-1}. Any control system could use online measurements of ρ, μ, and T at the location of the online monitoring devices along with a database of values for ρ_{water} and μ_{water} to solve the system of equations and calculate C_{CO_2} and C_{PZ} in real time.

The regression for μ was developed with only 8 *m* PZ data, and this limits its application. The viscosity of PZ solutions is complicated, and regressions across large PZ concentration ranges generally contain unacceptable levels of error for online monitoring applications. The regression of ρ was developed over (5 to 12) *m* PZ and should be very robust in applications centering around 8 *m* PZ, the most likely concentration of concentrated PZ systems. Coriolis type flowmeters have been reported to have accuracies of ± 1 kg·m^{-3} in the measurement of density while standard online viscometers have reported accuracies of 1 %. With accurate, simultaneous measurements of ρ and μ, the CO_2 and PZ concentrations of an 8 *m* PZ solution could be correlated to within 5 % and proved reliable, real-time monitoring of the solution composition.

AUTHOR INFORMATION

Corresponding Author

*E-mail: sfreeman@che.utexas.edu, gtr@che.utexas.edu.
Tel.: +1 (512) 471-7230. Fax: +1 (512) 471-7060.

Funding Sources

The Luminant Carbon Management Program provided support for this research.

REFERENCES

(1) Freeman, S. A.; Davis, J.; Rochelle, G. T. Degradation of aqueous piperazine in carbon dioxide capture. *Int. J. Greenhouse Gas Control* **2010**, *4*, 756–761.

(2) Freeman, S. A.; Dugas, R.; VanWagener, D.; Nguyen, T.; Rochelle, G. T. Carbon dioxide capture with concentrated, aqueous piperazine. *Int. J. Greenhouse Gas Control* **2010**, *4*, 119–124.

(3) Chen, E. Carbon Dioxide Absorption into Promoted Potassium Carbonate in Structured Packing. Ph.D. Dissertation, The University of Texas at Austin, Austin, TX, 2007.

(4) Dugas, R. E. Carbon Dioxide Absorption, Desorption, and Diffusion in Aqueous Piperazine and Monoethanolamine. Ph.D. Dissertation, The University of Texas at Austin, Austin, TX, 2009.

(5) Liu, H.-B.; Zhang, C.-F.; Xu, G.-W. A Study on Equilibrium Solubility for Carbon Dioxide in Methyldiethanolamine-Piperazine-Water Solution. *Ind. Eng. Chem. Res.* **1999**, *38*, 4032–4036.

(6) Paul, S.; Mandal, B. Density and viscosity of aqueous solutions of (N-methyldiethanolamine plus piperazine) and (2-amino-2-methyl-1-propanol plus piperazine) from (288 to 333) K. *J. Chem. Eng. Data* **2006**, *51*, 1808–1810.

(7) Bishnoi, S.; Rochelle, G. T. Physical and chemical solubility of carbon dioxide in aqueous methyldiethanolamine. *Fluid Phase Equilib.* **2000**, *168*, 241–258.

(8) Bishnoi, S.; Rochelle, G. T. Absorption of carbon dioxide into aqueous piperazine: reaction kinetics, mass transfer and solubility. *Chem. Eng. Sci.* **2000**, *55*, 5531–5543.

(9) Bishnoi, S.; Rochelle, G. T. Thermodynamics of piperazine/methyldiethanolamine/water/carbon dioxide. *Ind. Eng. Chem. Res.* **2002**, *41*, 604–612.

(10) Bishnoi, S.; Rochelle, G. T. Absorption of carbon dioxide in aqueous piperazine/methyldiethanolamine. *AIChE J.* **2002**, *48*, 2788–2799.

(11) Zhang, X.; Zhang, C. F.; Qin, S. J.; Zheng, Z. S. A kinetics study on the absorption of carbon dioxide into a mixed aqueous solution of methyldiethanolamine and piperazine. *Ind. Eng. Chem. Res.* **2001**, *40*, 3785–3791.

(12) Derks, P. W. J.; Hamborg, E. S.; Hogendoorn, J. A.; Niederer, J. P. M.; Versteeg, G. F. Densities, viscosities, and liquid diffusivities in aqueous piperazine and aqueous (piperazine plus N-methyldiethanolamine) solutions. *J. Chem. Eng. Data* **2008**, *53*, 1179–1185.

(13) Samanta, A.; Bandyopadhyay, S. S. Absorption of carbon dioxide into aqueous solutions of piperazine activated 2-amino-2-methyl-1-propanol. *Chem. Eng. Sci.* **2009**, *64*, 1185–1194.

(14) Sun, W. C.; Yong, C. B.; Li, M. H. Kinetics of the absorption of carbon dioxide into mixed aqueous solutions of 2-amino-2-methyl-l-propanol and piperazine. *Chem. Eng. Sci.* **2005**, *60*, 503–516.

(15) Yang, Z.-Y.; Soriano, A. N.; Caparanga, A. R.; Li, M.-H. Equilibrium solubility of carbon dioxide in (2-amino-2-methyl-1-propanol + piperazine + water). *J. Chem. Thermodyn.* **2010**, *42*, 659–665.

(16) Oyenekan, B. A.; Rochelle, G. T. Rate modeling of CO_2 stripping from potassium carbonate promoted by piperazine. *Int. J. Greenhouse Gas Control* **2009**, *3*, 121–132.

(17) Cullinane, J. T.; Rochelle, G. T. Carbon dioxide absorption with aqueous potassium carbonate promoted by piperazine. *Chem. Eng. Sci.* **2004**, *59*, 3619–3630.

(18) Cullinane, J. T.; Rochelle, G. T. Thermodynamics of aqueous potassium carbonate, piperazine, and carbon dioxide. *Fluid Phase Equilib.* **2005**, *227*, 197–213.

(19) Cullinane, J. T.; Rochelle, G. T. Kinetics of carbon dioxide absorption into aqueous potassium carbonate and piperazine. *Ind. Eng. Chem. Res.* **2006**, *45*, 2531–2545.

(20) Plaza, J. M.; Chen, E.; Rochelle, G. T. Absorber intercooling in CO_2 absorption by piperazine-promoted potassium carbonate. *AIChE J.* **2009**, *56*, 905–914.

(21) Rochelle, G. T. Amine Scrubbing for CO_2 Capture. *Science* **2009**, *325*, 1652–1654.

(22) *Ethyleneamines*; The Dow Chemical Company: Midland, MI, 2001; p 48.

(23) Hilliard, M. D. *A Predictive Thermodynamic Model for an Aqueous Blend of Potassium Carbonate, Piperazine, and Monoethanolamine for Carbon Dioxide Capture from Flue Gas*; The University of Texas at Austin: Austin, TX, 2008.

(24) Cook, H. L.; Lowe, B. M. Viscosity B-Coefficients for Pinacol and Piperazine in Aqueous-Solution at 25 and 35 °C. *Electrochim. Acta* **1976**, *21*, 153–154.

(25) Derks, P. W.; Hogendoorn, K. J.; Versteeg, G. F. Solubility of N_2O in and density, viscosity, and surface tension of aqueous piperazine solutions. *J. Chem. Eng. Data* **2005**, *50*, 1947–1950.

(26) Muhammad, A.; Mutalib, M. I. A.; Murugesan, T.; Shafeeq, A. Thermophysical Properties of Aqueous Piperazine and Aqueous (N-Methyldiethanolamine plus Piperazine) Solutions at Temperatures (298.15 to 338.15) K. *J. Chem. Eng. Data* **2009**, *54*, 2317–2321.

(27) Samanta, A.; Bandyopadhyay, S. S. Density and viscosity of aqueous solutions of piperazine and (2-amino-2-methyl-1-propanol + piperazine) from 298 to 333 K. *J. Chem. Eng. Data* **2006**, *51*, 467–470.

(28) Samanta, A.; Roy, S.; Bandyopadhyay, S. S. Physical solubility and diffusivity of N_2O and CO_2 in aqueous solutions of piperazine and (N-methyldiethanolamine plus piperazine). *J. Chem. Eng. Data* **2007**, *52*, 1381–1385.

(29) *DIPPR 801 Database of Physical and Thermodynamic Properties of Pure Chemicals*; Brigham Young University; http://dippr.byu.edu/public/chemsearch.asp (accessed March 1, 2010).